
Experimental determination of moments of inertia for an off-road vehicle in a regular engineering laboratory

P. E. Uys (corresponding author), P. S. Els, M. J. Thoresson, K. G. Voigt and W. C. Combrinck
Department of Mechanical and Aeronautical Engineering, University of Pretoria, Pretoria, 0002, South Africa
E-mail: petro.uys@up.ac.za

Abstract Moments of inertia play a vital role in the motion of rigid bodies. Accurate information for moments of inertia is, however, not easily obtained for common bodies such as vehicles, aeroplanes, trains and humans. Presented in this text is a procedure, requiring minimal equipment expenditure, for the determination of the moments of inertia, for an off-road vehicle. The point of departure is rigid-body oscillation about a pivoting point, with a spring providing a restoring force. The moment of inertia about the pivoting point is then determined by both measuring the period of oscillation and calculating the gradient of the torque–angular acceleration curve. The results of the two methods for determining the pitch, roll and yaw moments of inertia of the body and chassis about the body's centre of gravity are compared. It is found that calculation is very sensitive to distance measurements and accurate determination of the position of the centre of gravity. The procedure gives results of adequate accuracy considering the experimental effort and costs involved.

Keywords moment of inertia; vehicle dynamics; roll; pitch; yaw

Notation

b	horizontal distance c.o.g. to rear hub centre (m)
c.o.g.	centre of gravity
F	force (N)
F_{spring}	spring force (N)
g	gravitational acceleration (9.81 m/s ²)
H	distance tyre lowest point to force point of application for determining c.o.g. (m)
h	height of c.o.g. (m)
\bar{I}	moment of inertia of item with respect to an axis passing through the centres of gravity and parallel to the axis of rotation
I_{axle}	moment of inertia of axle, kg m ²
\bar{I}_{beam}	moment of inertia of beam, kg m ²
I_o	the moment of inertia about the axis of rotation (kg m ²)
$\bar{I}_{\text{body}}^{\text{pitch}}$	pitch moment of inertia of the vehicle body and chassis about its centre of gravity (kg m ²)
$\bar{I}_{\text{body}}^{\text{roll}}$	roll moment of inertia of the vehicle body and chassis about its centre of gravity (kg m ²)
$\bar{I}_{\text{body}}^{\text{yaw}}$	yaw moment of inertia of the vehicle body and chassis about its centre of gravity (kg m ²)

k	spring stiffness coefficient (N/m)
L	wheelbase for determining c.o.g
L_{acc}	distance accelerometer to pivoting point
L_{beam}	rectilinear distances between the axis of rotation and beam c.o.g. (m)
L_{displ}	distance of displacement sensor from pivoting point O (m)
L_{force}	distance of the spring from pivoting point O (m)
L_{j_axle}	rectilinear distances between the axis of rotation and axle c.o.g. (m), j = rear or front
$L_{rotax_cog_body}$	rectilinear distance from c.o.g. of body to pivoting point (m)
m	total vehicle mass (kg)
m_{axle}	mass of axle (kg)
m_{beam}	mass of beam (kg)
m_{body}	mass of vehicle body and chassis (kg)
m_{wheel}	mass of wheel
R	rear wheel-ground contact point
T_o	torque about pivoting point O (Nm)
T_R	torque about pivoting point R (Nm)
x	linear displacement (m)
x_F	$= \frac{L_{force}}{L_{displ}}x$, displacement of spring (m)
\ddot{x}	lateral acceleration (m/s ²)
δ	$= \ln \frac{x_1}{x_2}$, logarithmic decrement, x_1 and x_2 displacement amplitudes of consecutive oscillations
ζ	$= \frac{\delta^2}{\sqrt{\delta^2 + (2\pi)^2}}$, damping ratio
θ	angular displacement (rad)
$\ddot{\theta}$	angular acceleration (rad/s ²)
ΣT_o	sum of the moments of the external forces about point O (Nm)
τ	natural period of free vibration of spring (s)
τ_d	damped period (s)
ω_n	undamped natural frequency (rad/s)
ω_d	damped frequency (rad/s)

Introduction

The performance of a vehicle's suspension is judged in terms of ride comfort, handling and stability. Ride comfort is an expression of human experience of the road input to the vehicle, as perceived in terms of vibration and motion sickness. While vertical acceleration is regarded as an accurate metric of discomfort originating from higher frequencies [1], low-frequency discomfort (normally motion sickness) is related to vehicle pitching [2]. Handling, on the other hand, describes the cornering and road-holding capability of a vehicle. The handling performance of a vehicle is thus dependent on tyre characteristics, lateral and yaw motion (i.e. rotation about a

vertical axis) and the amount of roll experienced by the vehicle about a longitudinal axis due to suspension movement. Stability concerns not only road-holding capability but also roll-over propensity, which is to a large extent determined by roll velocity and acceleration, the height/width ratio of the vehicle, as well as the roll moment of inertia. The pitch, yaw and roll moments of inertia are therefore of utmost importance for determining actual and perceived vehicle behaviour.

Several methods have been suggested for determining inertial properties. Some methods use specially designed equipment and therefore require a large capital layout. Other methods are straightforward, but require considerable data reduction and interpretation expertise. Ringeagni *et al.* [3] describe the use of a torsional pendulum to determine mass inertial properties of irregularly shaped bodies. The pendulum consists of a movable aluminium-foam-aluminium composite disc hanging from another properly aligned similar disc by means of three steel wires placed 120° from one another. The centre of gravity of the body, for which the moments of inertia are to be determined, is placed equidistant from all the wires. Accurate calibration of the pendulum in terms of its geometrical characteristics is necessary to obtain trustworthy results. The method was used to determine properties of satellite components and assemblies.

Schedlinski and Link [4] did a survey of inertia parameter identification methods. They refer to the use of a robot providing spatial motion from which both products and moments of inertia of bodies with limited size can be obtained. A run-down method is described where a specimen is rotated about an axis coinciding with the vertical axis of the body fixed frame and the inertia frame. The rotational acceleration and torque are measured for different rotation velocities, but there is a high risk of damage due to rotational acceleration. Offsetting the centre of gravity and using a similar device with rotation at constant speed, products of inertia can be calculated by means of dynamic balancing. The same authors refer to the use of the gravitational pendulum method, where test specimens are supported by knife-edges or suspended wires. A physical pendulum is thus created, with gravitation as the restoring torque. For a known location of the centre of gravity, the moment of inertia about the pendulum axis is obtained by measuring the oscillation frequencies. Schedlinski and Link [4] note that the procedure is safe, has been approved by industry and requires simple software and basic skills, but that the accuracy is unknown and the data-processing requirements high. The same authors also mention measurement by means of the torsional pendulum method, with the rotation axis, z -axis of the inertial frame and an axis of the body fixed frame coinciding, the restoring torque being generated by springs. This can be repeated for other axes. If the rotation axes intersect at a single point, the inertia tensor can be obtained. The method has high accuracy. If wires suspend the specimen, the wires create a restoring moment. Hardware requirements are extensive, especially for large masses. This method is applied by industry. Time requirements are high, as is accuracy, and the method is safe if the suspension is secure.

Another approach [4] is to excite all the translational and rotational motions of a mechanical system and to use modal analysis for determining moments of inertia. Measurements of accelerations, forces and torques are required and all nine inertia

properties and the position of the centre of gravity can be obtained simultaneously. An increase in the number of parameters to be identified may result in less accuracy, but improved accuracy can be achieved if the mass and centre of gravity are known beforehand, from static tests. The method is safe if excitation forces are kept low. The system must be resiliently suspended and modal testing and signal-processing equipment is required, while skill requirements are high. Time requirements are medium and accuracy deviations vary from 10% to 20%. Alternatively, direct physical parameter identification methods focusing on a fit of system matrices to measured vibration response data can be used. In this case deviations of 0.5% to 8% are mentioned.

The pendulum method has been used since the 1930s to determine the moments of inertia of aeroplanes [5]. A bifilar type of pendulum is used to determine the yaw moment of inertia. The axis of oscillation is vertical, lies midway between the vertical filaments and passes through the centre of gravity of the system. For the compound pendulum used in determination of the roll and pitch moments of inertia, the axis of oscillation is horizontal and passes through points of support but not through the centre of gravity. Damping causes an estimated error of less than 2%. Due to the relative low mass density of aeroplanes, the additional-mass effects due to the buoyancy of the structure, the air entrapped in the structure and the momentum imparted on the surrounding air due to the motion of the body, need to be taken into account. Errors of 0.8%, 1.3% and 2.5% are claimed for the yaw, pitch and roll axes, respectively. The greater precision of the first arises from the fact that no transposition of the axis is necessary. Difficulties encountered include ensuring that rotation is about a single well defined axis; that is, the structure should be sufficiently rigid and the pivoting points carefully constructed. Measurement of the compound length and thus the period of oscillation is dependent on accurate determination of the centre of gravity.

From a bio-medical point of view, an oscillating table was used to determine the moments of inertia in adolescent boys [6]. The table floats on compressed air to reduce friction and rotation is counteracted by a compressed spring. A body of known moment of inertia is oscillated using a small angle, so that linearisation applies, to calculate the physical parameters of the system. A body's moment of inertia about the axis of oscillation is then determined in terms of the measured period of the oscillating table itself and the period of oscillation of the body. The moment of inertia relative to the centre of gravity can be obtained using the parallel axis theorem. By these means the relation between moment of inertia, body weight and length is obtained.

Using free damped oscillations induced by an initial displacement or velocity, Wu and Hsieh [7] were able to determine mass moments of inertia for a floating body in heave and pitch while also accounting for added mass due to buoyancy.

The determination of the moments of inertia of heavy military vehicles by means of torsional oscillation, for the US Army Tank–Automotive and Armaments Command, is described by Andreatta *et al.* [8]. They describe a permanent facility consisting of a multiple-piece platform with a steel truss design with aluminium decking sections that can be adjusted. The pivot is above the centre of gravity of the

system so that gravity rather than springs provide restoring forces for roll and pitch. Rails make selection of different pivoting points possible. A rotation angle of 3° to 3.5° is given to the platform and the period of oscillation measured. For yaw, the platform assembly rotates on a turntable bearing and is constrained by yaw springs. The system thus acts as a torsional pendulum. Vehicles ranging in mass from 1360 kg to 27 000 kg can be accommodated. This system, however, requires considerable capital layout.

On the vehicle side, the design of a measurement facility to determine inertia parameters is discussed by Heydinger *et al.* [9]. The facility consists of an oscillating platform equipped with pylons and a yaw/roll assembly that supports the platform during roll, yaw and roll–yaw product of inertia determination. In the design, the following considerations have been accounted for from previous experience. First, major sources of error result from platform deflection, roll moment of inertia of the test device itself, non-linear springs, the pivot height and the distance between the pivot and the combined centre of gravity, which affects the period of oscillation. Second, there is a trade-off between the short oscillation periods (high acceleration) and long oscillation periods (low acceleration). The roll–yaw product of inertia is considered a necessary inertia parameter to be measured due to its influence on vehicle response.

Bixel *et al.* [10] describe methods that can be used to estimate vehicle moments of inertia by using easily measurable values such as the height of the centre of gravity, the roof height and track width. Approximation constants based on National Highway and Safety Administration data for over 300 vehicles are incorporated in the formulas that apply to post-1980 vehicles. MacInnis *et al.* [11] compare several estimation model results with measured data.

In order to measure the inertia tensor, a rig that consisted of a four-bar pendulum and carrying the rigid body by means of a rigid frame was used by Doniselli *et al.* [12]. Measurements were by means of accelerometers, gyroscopes and inclinometers.

Sharp [13] describes the derivation of moments of inertia and centre of gravity by mounting a large hemispherical bearing on a garage hydraulic lift and adding a subsidiary bearing concentric with the hydraulic arm for a yaw axis. Symmetry is no longer assumed and the principal moments and inertia axis can be determined.

Background

Although the methods described in the previous section relate to simple basic dynamics theory, the equipment to determine the moments of inertia of the different objects is rather complex and expensive, and requires skilled technicians and adequate signal-processing equipment. In a regular university engineering faculty laboratory, where vehicle dynamics is but one topic among a variety of fields of interest, such equipment is seldom available. Ingenious methods have to be developed which are cost-effective and accurate enough for control-related simulations. The drive for the initiative reported on here, arose from a discrepancy in the simulated and measured handling behaviour of a two-ton LandRover Defender used in

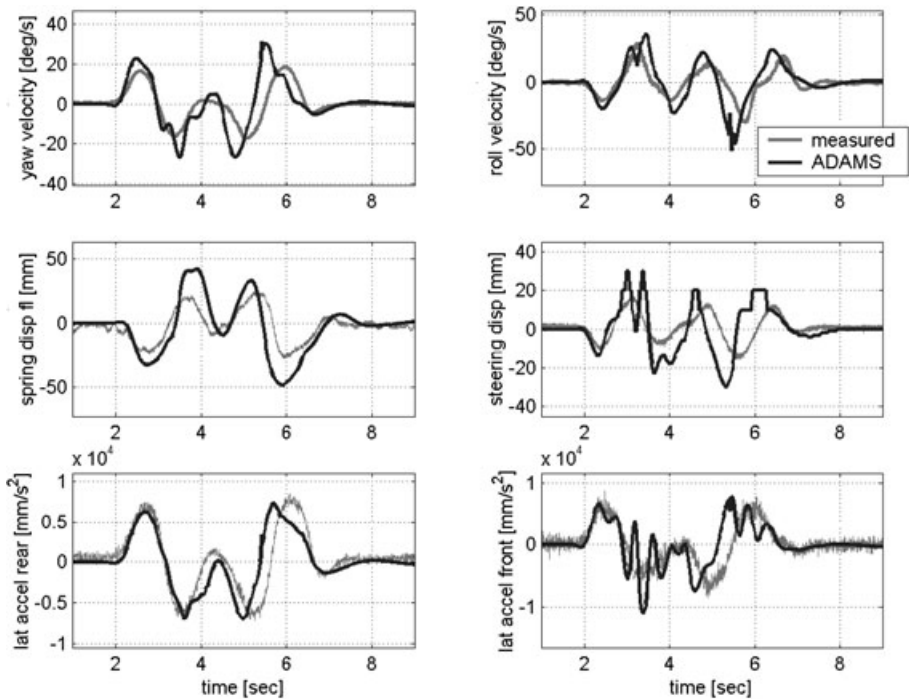


Fig. 1 Vehicle model validation results for a double lane change.

the development of a semi-active suspension system. Fig. 1 compares the simulation results obtained from ADAMS software and the measured data. Discrepancies with respect to the lateral dynamics could partially be attributed to the driver model and inaccurate values for centre of gravity and moments of inertia. Better estimates of these parameters were thus required.

Accelerometers, displacement transducers, load cells and field test signal-processing equipment were available. Determination of moments of inertia using the rotational vibration of a rigid body about a pivoting point, with a restoring force provided by a spring, thus seemed the most feasible approach.

In terms of vehicle simulation requirements, roll, pitch and yaw moments of inertia about the vehicle's longitudinal, lateral and vertical axes (Fig. 2) are the most important inertia parameters and the focus is thus on determining these. In order to apply the equations pertaining to a rigid body oscillating about a pivoting point, the vehicle had to be converted to a rigid body, and so suspension compliance was eliminated. This was done by fixing a rigid rod, of length equal to the static length of the damper, between the chassis and the axle. This also kept the position of the centre of gravity constant.

For undamped free vibration of a rigid body in a plane, pivoting about point O, as presented in Fig. 3, the generalised form of Newton's second law can be applied:

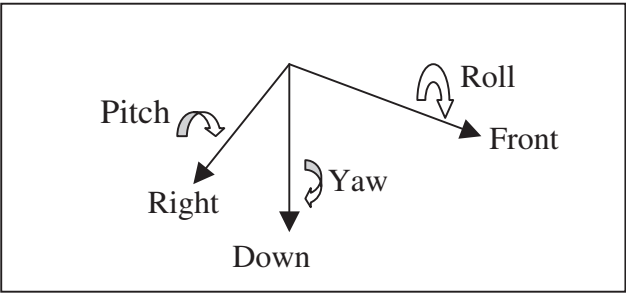


Fig. 2 Vehicle axis system.

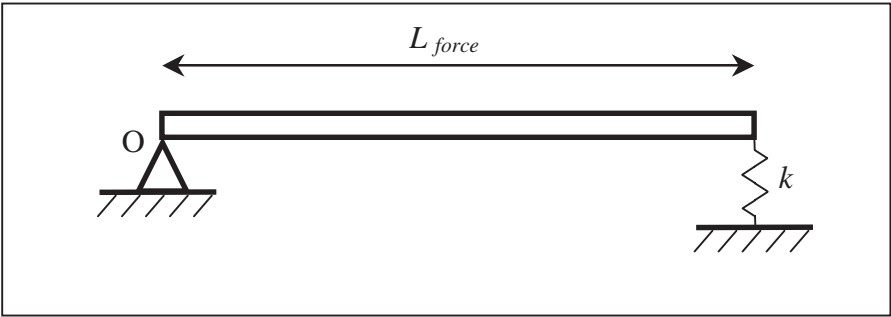


Fig. 3 Schematic presentation of the rotational vibration of a rigid body.

$$\Sigma T_o = I_o \ddot{\theta} \tag{1}$$

where $\ddot{\theta}$ is the angular acceleration, ΣT_o is the sum of the moments of the external forces about O and I_o is the moment of inertia about the axis of rotation.

The force, $kx = kL_{force} \sin \theta$, induced by the spring, of stiffness coefficient k , due to lengthening or compression by a distance x for an angular displacement θ , creates a restoring moment, $kL_{force}^2 \sin \theta \cos \theta$, about point O. For small rotational displacements $\sin \theta \sim \theta$ and $\cos \theta \sim 1$ and consequently the restoring moment can be approximated by:

$$\Sigma T_o = -kL_{force}^2 \theta \tag{2}$$

After this linearisation the equation of motion (1) is obtained as:

$$\ddot{\theta} + \frac{kL_{force}^2}{I_o} \theta = 0 \tag{3}$$

where displacement from the equilibrium position is considered and

$$\omega_n = \sqrt{\frac{kL^2}{I_o}} \text{ (in rad/s)} \tag{4}$$

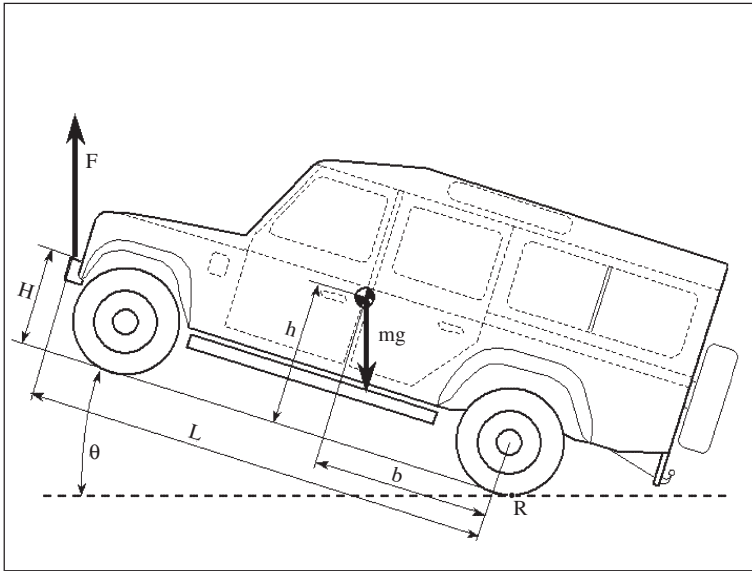


Fig. 4 Obtaining the position of the centre of gravity.

is the undamped natural frequency of the system.

The period of free vibration in seconds is thus given by:

$$\tau = 2\pi \sqrt{\left(\frac{I_o}{kL_{\text{force}}^2} \right)} \quad (5)$$

By measuring the period of oscillation, the moment of inertia can be obtained for known spring stiffness:

$$I_o = \frac{\tau^2 kL_{\text{force}}^2}{(2\pi)^2} \quad (6)$$

Using a bifilar or compound pendulum approach results in a similar equation. The construction of a suitable pendulum or an oscillating platform on which objects with considerable mass and geometry, such as the two-ton LandRover under discussion, can be mounted, would be expensive and time consuming. Therefore a more direct approach was used. The experimental procedure pursued to determine the position of the centre of gravity and the pitch, yaw and roll moments of inertia of the vehicle is presented in the following section.

Determining the position of the centre of gravity

The position of the centre of gravity was obtained by fixing the rear wheels to prevent motion, and by lifting the front end with a crane, using a measured force, F , until the vehicle made an angle θ with the horizontal (Fig. 4).

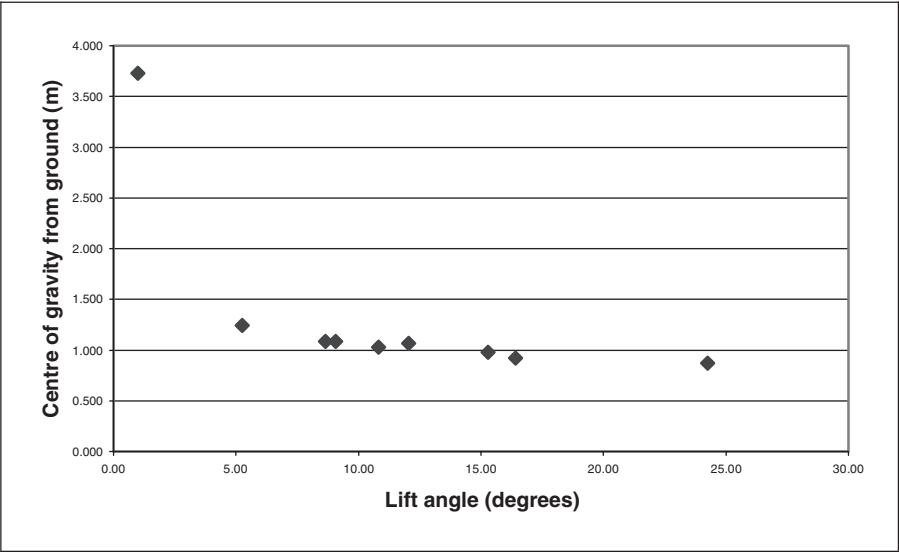


Fig. 5 Results from centre-of-gravity determination.

TABLE 1 Inertia properties of vehicle items

Item	Property
Mass of wheel	31.5 kg
Mass of axle	166 kg
Mass of body and chassis	1567 kg
Mass of vehicle	2025 kg
Mass of beam used for roll moment of inertia	105 kg
c.o.g. roll moment of inertia for beam	0.634 kg m ²
c.o.g. roll moment of inertia for axles	33.1 kg m ²

Taking moments about the rear wheel–ground contact point, R, and equating to zero, results in equation 7:

$$\Sigma T_R = LF \cos \theta - HF \sin \theta - mgb \cos \theta + mgh \sin \theta = 0 \tag{7}$$

After obtaining b from the values at $\theta = 0^\circ$, equation 7 can be solved for h . Fig. 5 depicts the results obtained for different angles. As the angle is increased, the accuracy of the method improves, and the height of the centre of gravity stabilises at a value of $h = 1.003\text{ m}$ from the ground.

The masses of the wheels and axles are given in Table 1. The location of the centre of gravity of the vehicle and body and the geometry pertaining to the experimental configurations are shown in Fig. 6. In the calculation, the vehicle is considered to be symmetrical in the horizontal direction and the centre of gravity located in the

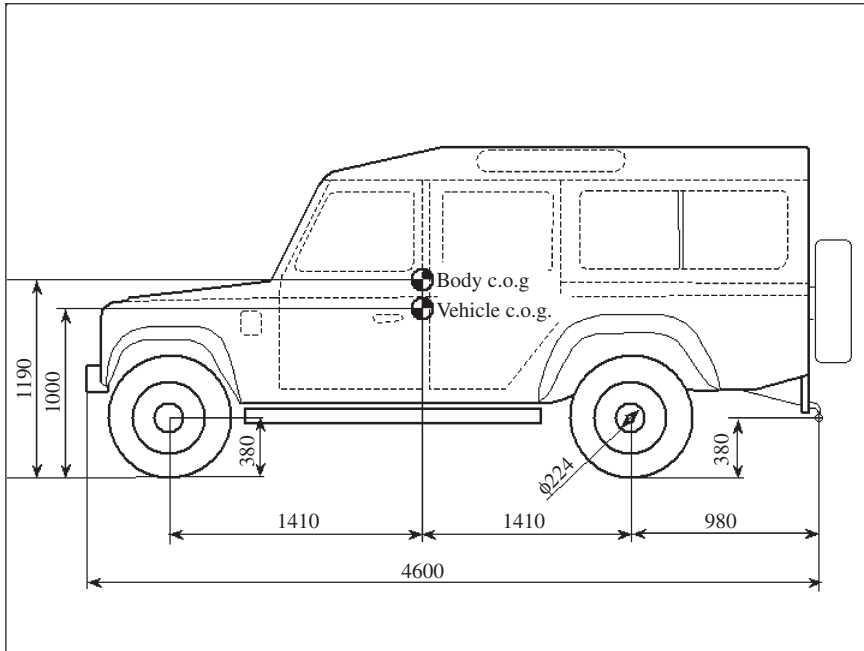


Fig. 6 Location of centres of gravity and vehicle geometry.

midplane. The symmetry of the mass distribution holds, although the vehicle components may not be completely symmetric.

Pitch moment of inertia

The moments of inertia needed for simulation purposes are those of the vehicle body and of the chassis, excluding the wheels and axles. Two wheels, but no axles, were removed due to the difficulty and time implications of removing the latter. It is also necessary to remove the rear wheels to prevent rolling about the wheels when the vehicle is pivoted about the rear axle *O* (Fig. 7). The front wheels were retained for safety reasons. The presence of the axles and front wheels has been accounted for in the final calculation, as indicated below. A spring is mounted between the floor and the front bumper (at *C* in Fig. 7) to provide the restoring moment. The rear hubs, *O*, are placed on knife-edges supported by trestles. A load cell (at *C* in Fig. 7), a displacement transducer (at *B* in Fig. 7), and also an accelerometer (at *A* in Fig. 7) are mounted to the system. A small vertical perturbation is given at the front. The system oscillates about the rear axle. The period of oscillation, τ , as well as the displacement, x , lateral acceleration, \ddot{x} , and force, F , are registered. The actual set-up can be seen in Fig. 8.

From the theory previously presented, it follows that the moment of inertia is given by:

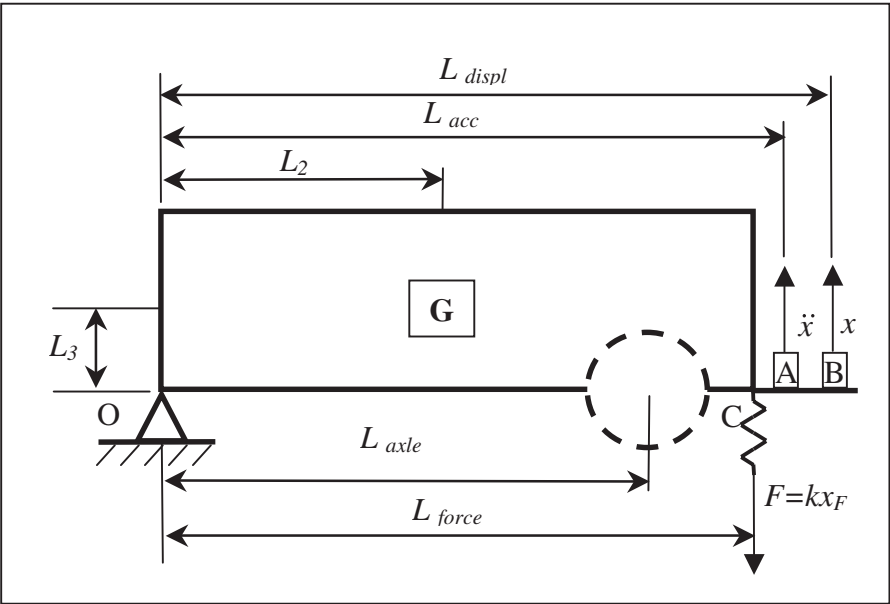


Fig. 7 Schematic presentation of the experimental set-up for pitch.

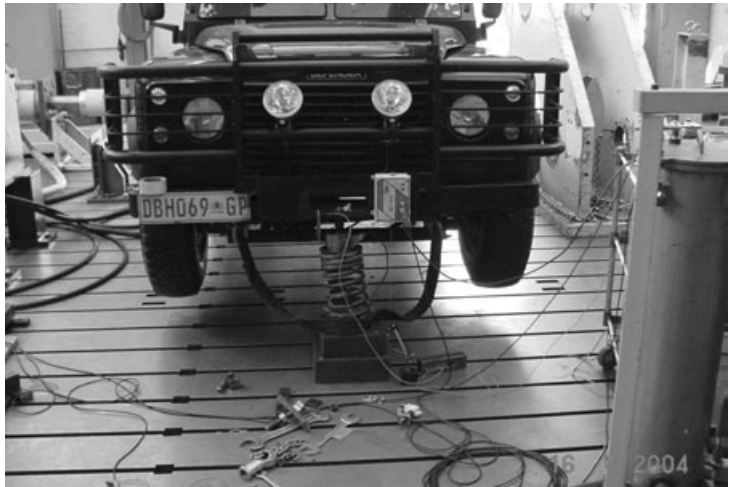


Fig. 8 Experimental configuration for determining pitch moment of inertia.

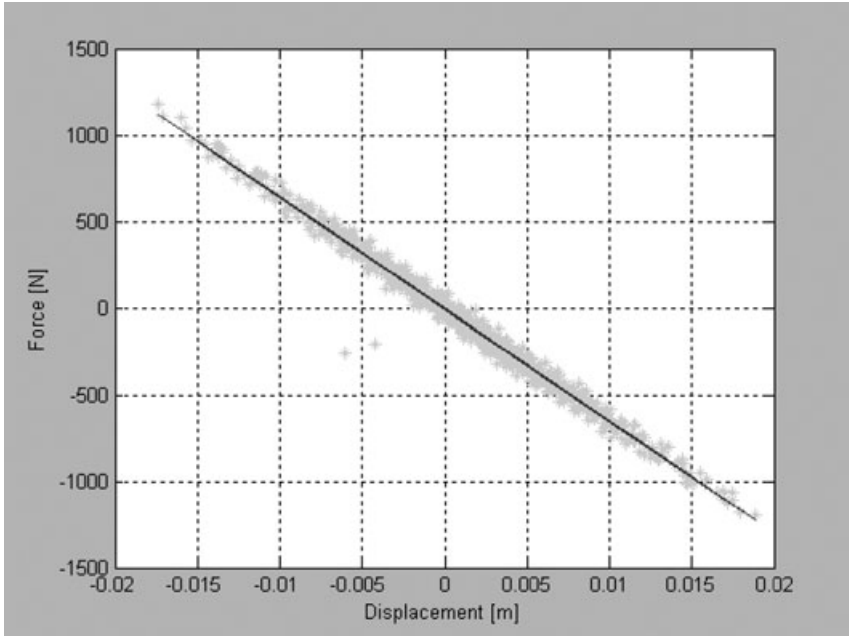


Fig. 9 Force versus displacement for pitch oscillation.

$$I_o = \frac{\tau^2 k L_{\text{force}}^2}{2\pi} \quad (8)$$

In order to determine I_o , the spring stiffness, k , must be known. The stiffness can be obtained from the measured displacement (x) and the corresponding spring force (F_{spring}). The spring stiffness is obtained from the gradient of the $F_{\text{spring}} - x$ graph linearised about the static position (Fig. 9).

When plotting the force–displacement curve, care should be taken that the displacement of the displacement transducer at distance L_{displ} from O with respect to the distance of the spring from O, L_{force} , is accounted for (see Fig. 10):

$$x_F = \frac{L_{\text{force}}}{L_{\text{displ}}} x \quad (9)$$

Another approach is to obtain the angular acceleration, $\ddot{\theta}$, from the linear acceleration, \ddot{x}_F , at the point of application of the force:

$$\ddot{\theta} = \frac{\ddot{x}_F}{L_{\text{acc}}} \quad (10)$$

From equation 1 it is apparent that plotting the torque, $T = -F_{\text{spring}} L_{\text{force}}$, where F_{spring} is measured by means of the load cell, against the angular acceleration obtained from

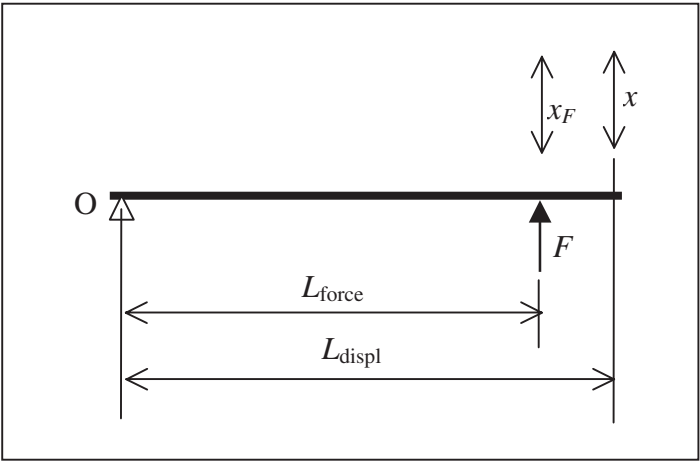


Fig. 10 Location of displacement transducer with respect to the work line of the force.

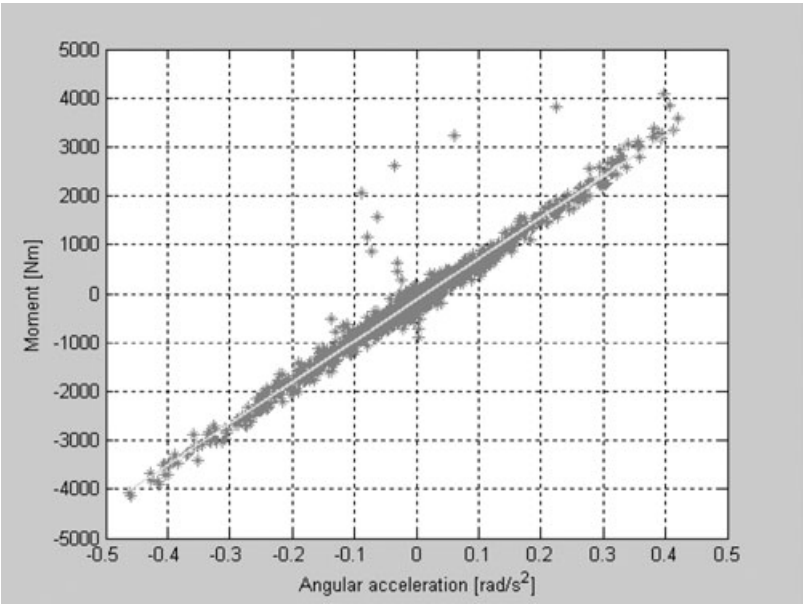


Fig. 11 Moment versus angular acceleration for pitch oscillation.

the acceleration measured by the accelerometer, the moment of inertia can be obtained from the gradient of the $T - \ddot{\theta}$ curve (Fig. 11).

Furthermore, there is some damping present in the system, as can be seen from Fig. 12. Consequently, the period that is measured is the damped period and not

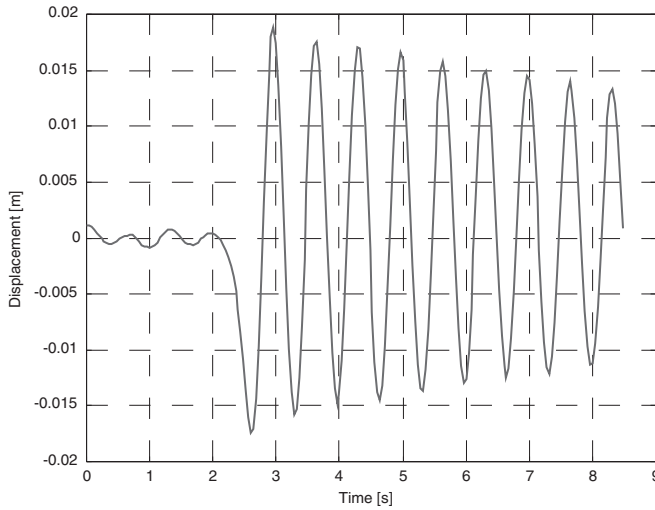


Fig. 12 Displacement–time graph for pitch oscillation.

the period related to the natural frequency of the system, as is required by equation 8.

Referring to the displacement–time graph (Fig. 12), the logarithmic decrement, δ , is determined from the relation:

$$\delta = \ln \frac{x_1}{x_2} \quad (11)$$

where x_1 is the amplitude of the first oscillation and x_2 of the following one. The damping ratio is:

$$\zeta = \frac{\delta^2}{\sqrt{\delta^2 + (2\pi)^2}} \quad (12)$$

and the natural period, τ , then follows from the observed damped period, τ_d , using the relation:

$$\tau = \sqrt{1 - \zeta^2} \tau_d \quad (13)$$

The corresponding natural circular frequency is given by:

$$\omega_n = \omega_d \frac{1}{\sqrt{1 - \zeta^2}} \quad (14)$$

where ω_d is the damped circular frequency.

The average damping ratio obtained amounted to 0.011. There was a negligible difference between the damped and undamped frequencies, and the average stiffness coefficient was found to be 64 882 N/m, linearised about the static position.

TABLE 2 Pitch moment-of-inertia results

Dataset	10	9	8	7	Average
I_o (accelerometer), kg m^2	8431	8280	8435	8453	8400
$\bar{I}_{\text{body}}^{\text{pitch}}$ (accelerometer), kg m^2	2472	2321	2475	2493	2440
I_o (period spring), kg m^2	9185	8675	9162	10 172	9298
$\bar{I}_{\text{body}}^{\text{pitch}}$ (period spring), kg m^2	3226	2715	3202	4 212	3339
ω_{d} , rad/s	9.18	9.47	9.21	8.74	9.15
ζ	0.008	0.012	0.007	0.016	0.011

To derive the pitch moment of inertia of the vehicle body without the axles, $\bar{I}_{\text{body}}^{\text{pitch}}$, about the centre of gravity, the parallel axis theorem is used:

$$\bar{I}_{\text{body}}^{\text{pitch}} = I_o - m_{\text{body}}(L_2^2 + L_3^2) - (m_{\text{axle}} + 2m_{\text{wheel}})L_{\text{axle}}^2 \tag{15}$$

(The moment of the axle about its longitudinal axis is neglected.)

The results obtained by using the period and vertical acceleration measurements are given in Table 2. The average value obtained for the pitch moment of inertia about an axis passing through the body’s centre of gravity for a Land Rover Defender with a mass of 2025 kg is 3339 kg m², when determined by the period method. Using the gradient of the moment–angular acceleration curve gives a value of 2440 kg m² – a difference of almost 30%.

Discussion of results of pitch moment of inertia

The moment of inertia about the pivoting point, I_o , as determined by differentiating the results of the displacement transducer to determine the angular acceleration, differs about 0.5% from the same inertia moment determined with the accelerometer. This results in a 1.6% difference in the body moment of inertia, $\bar{I}_{\text{body}}^{\text{pitch}}$. As the accelerometer measurement was considered more direct, the related values were used for further comparison. Also, the moment of inertia determined about the pivoting point using the moment–angular acceleration, $T - \ddot{\theta}$, gradient, differed by 10% from that using the period. Because of the large contribution of the terms subtracted in equation 15, the 10% difference in the value of the moment of inertia about the pivoting point, I_o , results in a 30% difference for the moments of inertia about the body centre-of-gravity axis.

The difference in the moment-of-inertia results, when the two calculating methods are compared, may be ascribed to the effect of a friction moment induced at the pivoting point. This friction moment would be accounted for in the period measurement but not in the torque–acceleration curve, where the only moment considered is that due to the restoring force of the spring. Values obtained by measurement of the period should thus be considered the more accurate values. The large difference in the values about the centre-of-gravity axis furthermore indicates that the pivoting point should be as close as possible to the centre of gravity.

TABLE 3 Sensitivity of pitch moment-of-inertia calculations to parameter variation

Parameter varied	Baseline value	10% deviation in I_o (acc)	10% deviation in $L_{\text{rotax_cog_body}}$	10% deviation in k	10% deviation in L_{force}	10% deviation in ω_d
I_o (accelerometer)	8431.2	10	0	0	0	0
$\bar{I}_{\text{body}}^{\text{pitch}}$ (accelerometer)	2471.7	34	−35	0	0	0
I_o (period)	9185.2	0	0	10	21	−17
$\bar{I}_{\text{body}}^{\text{pitch}}$ (period)	3225.7	0	−27	28	60	−49
ω_d	9.2	0	0	0	0	10
ω_h	9.2	0	0	0	0	10
$L_{\text{rotax_cog_body}}$	1.6	0	10	0	0	0
L_{force}	3.5	0	0	0	10	0
k	64683	0	0	10	0	0

Table 3 summarizes the effect of variations in measurement of the position of the centre of gravity, the measured period, the spring coefficient and the measured position of the spring on the moment of inertia. It is apparent that a deviation of 10% in the measurement of the position of the centre of gravity with respect to the rotating axis ($L_{\text{rotax_cog_body}}$) results in an error of 27% in the body moment of inertia about its centre-of-gravity axis, due to the second term in equation 15. A 10% error in the position of the spring line of action causes a 21% deviation in the moment of inertia about the pivoting point I_o , as can be verified from equation 7. This error, however, causes a 60% error in the body centre-of-gravity moment of inertia, $\bar{I}_{\text{body}}^{\text{pitch}}$, which follows from the fact that the last two terms in equation 15 constitute some 60% of I_o . It is also apparent from Table 3 that $\bar{I}_{\text{body}}^{\text{pitch}}$ is very sensitive to errors in the spring coefficient (a 10% error causes a 28% error in $\bar{I}_{\text{body}}^{\text{pitch}}$) and period/frequency (a 10% error in ω_d results in a 49% error in $\bar{I}_{\text{body}}^{\text{pitch}}$).

Roll moment of inertia

The same principle as that used in the case of the pitch moment of inertia applies. The left front and rear hubs are placed on two V-grooves mounted on trestles. A universal beam is attached to the right front and rear hubs. The spring is placed between the centre of the universal beam and the floor. The vehicle is given a small vertical displacement to pivot about the supporting hubs (Fig. 13).

The equivalent of equation 15 for the roll moment of inertia is:

$$\bar{I}_{\text{body}}^{\text{roll}} = I_o - m_{\text{body}}(L_{\text{rotax_cog_body}}^2) - m_{\text{axle}}L_{\text{axle}}^2 - 2\bar{I}_{\text{axle}}\bar{I}_{\text{beam}} - m_{\text{beam}}L_{\text{beam}}^2 \tag{16}$$

In this case the moment of inertia of the axle about an axis perpendicular to the axle is not negligible (see Table 1). $L_{\text{rotax_cog_body}}$, L_{axle} and L_{beam} refer to the rectilinear distances between the axis of rotation and the body, axle and beam centres of gravity, respectively, while m_{body} , m_{axle} and m_{beam} are the corresponding masses. $\bar{I}_{\text{body}}^{\text{roll}}$, \bar{I}_{axle} and \bar{I}_{beam} are the respective moments of inertia of the body, axle and beam with respect

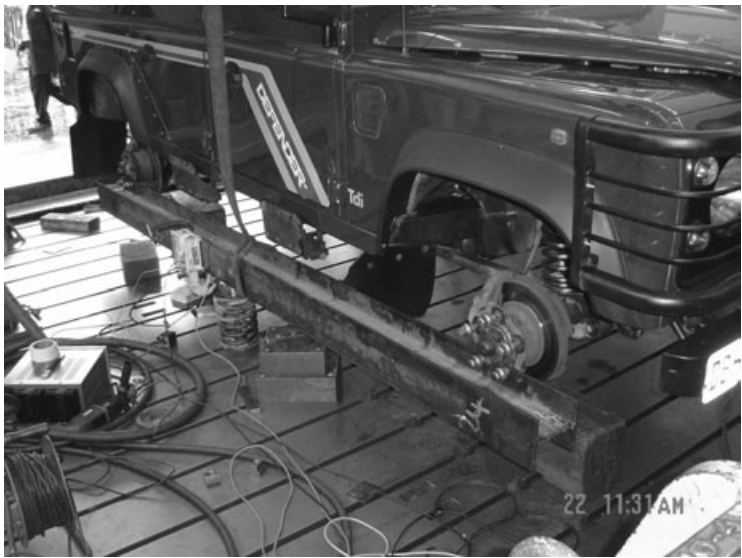


Fig. 13 Determining roll moment of inertia.

TABLE 4 Roll moment-of-inertia results

Dataset	2	3	4	5	Average
I_o (accelerometer), kg m^2	3862	3655	3557	3548	3655
$\bar{I}_{\text{body}}^{\text{roll}}$ (accelerometer), kg m^2	1046	838	741	731	839
I_o (period spring), kg m^2	3637	3549	3595	3463	3561
$\bar{I}_{\text{body}}^{\text{roll}}$ (period spring), kg m^2	820	733	779	646	744
τ , s	0.726	0.719	0.726	0.705	0.719
ζ	0.010	0.008	0.009	0.009	0.009

to an axis passing through their centres of gravity and parallel to the axis of rotation. The axles have been considered as slender rods with length equal to the axle length, 1.547 m, and \bar{I}_{beam} has been obtained from structural steel tables. The contribution of these two terms are $\bar{I}_{\text{axle}} = 33.1 \text{ kg m}^2$ for the axles and $\bar{I}_{\text{beam}} = 0.634 \text{ kg m}^2$ for the beam. The results related to different measurements are tabulated in Table 4. The average roll moment of inertia of the vehicle obtained from the data is 744 kg m^2 using the period and 839 kg m^2 using the torque angular acceleration gradient, a difference of 95 kg m^2 . The difference in moment of inertia about the pivoting point for the two methods is 2.6%.

A sensitivity analysis of the moments of inertia for different parameters has been conducted. The results are given in Table 5. The sensitivity to the distance from the rotation axis to the body centre of gravity axis, the distance to the action line of the

TABLE 5 Sensitivity of roll moment-of-inertia calculations to parameter variation

Parameter varied	Baseline value	10% deviation in I_o (acc)	10% deviation in $L_{\text{rotax_cog_body}}$	10% deviation in k	10% deviation in L_{force}	10% deviation in ω_d
I_o (accelerometer)	3557	10	0	0	0	0
$\bar{I}_{\text{body}}^{\text{roll}}$ (accelerometer)	741	48	−64	0	0	0
I_o (period spring)	3595	0	0	10	21	−17
$\bar{I}_{\text{body}}^{\text{roll}}$ (period spring)	779	0	−61	46	97	−80
ω_d	8.7	0	0	0	0	10
ω_h	8.7	0	0	0	0	10
$L_{\text{rotax_cog_body}}$	1.2	0	10	0	0	0
k	102414	0	0	10	0	0
L_{force}	1.622	0	0	0	10	0

spring and the value of the period is again apparent, as can be verified in terms of equations 6 and 15. Also, the difference in the values obtained from the torque–angular acceleration relation does not differ as much from that obtained by the period method (on average 11%) as is the case with the pitch moment of inertia (Table 3).

Yaw moment of inertia

Determining the yaw moment of inertia proved to be the most challenging task. For this purpose the tow bar was mounted upside down and supported on a pressure bearing (Fig. 14). In order to stabilise the vehicle overhead support was necessary (Fig. 15). This still proved to be inadequate to prevent roll. The problem was solved by attaching roller bearings, running horizontally on a mounted universal beam to ensure motion in the yaw plane, to the front bumper. A spring was mounted horizontally near the vertical height of the centre of gravity of the body (Fig. 16).

The moment of inertia can again be obtained both from the period and from the gradient of the torque–angular acceleration graph. Considerably more damping was present, as can be seen in Fig. 17.

The equivalent yaw moment of inertia for the body only is given by:

$$\bar{I}_{\text{body}}^{\text{yaw}} = I_o - m_{\text{body}}(L_{\text{rotax_cog_body}}^2) - (m_{\text{axle}} + 2m_{\text{wheel}})L_{\text{front_axle}}^2 - m_{\text{axle}}L_{\text{rear_axle}}^2 - 2\bar{I}_{\text{axle}} \quad (17)$$

Distances refer to the distances between the axis of rotation and axes passing through the centres of gravity and parallel to the rotational axis. An average value of 2057 kg m² was obtained for the yaw moment of inertia about the body centre-of-gravity with the torque–angular acceleration approach and 2478 kg m² using the period approach, as can be seen from Table 6, which summarises the results. The difference between the I_o values for the two different approaches is 2.7%.

From a more detailed investigation of the force–displacement curves (Fig. 18), it was apparent that the springs used in the various tests were not linear. While the

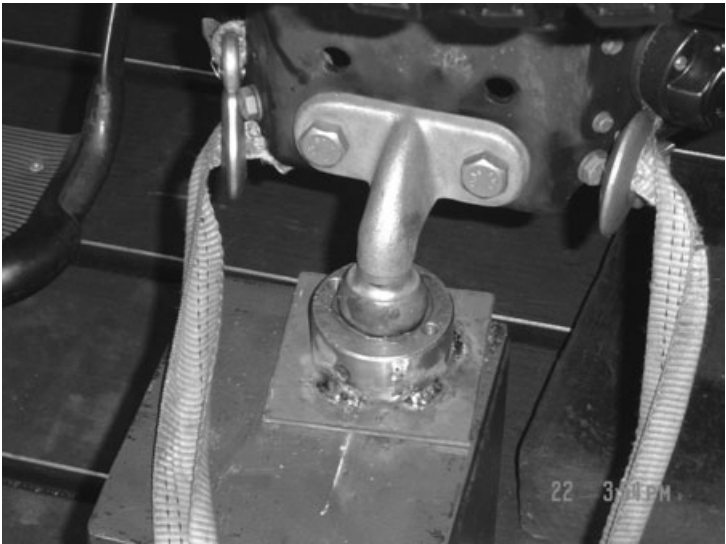


Fig. 14 The bearing and tow bar used for determining yaw moment of inertia.

TABLE 6 Yaw moment-of-inertia results

Dataset	5	6	7	8	9	Average
I_o (accelerometer), kg m^2	14029	14784	14969	14741	14770	14659
$\bar{I}_{\text{body}}^{\text{yaw}}$ (accelerometer), kg m^2	1428	2182	2368	2139	2169	2057
I_o (period), kg m^2	14476	15756	14542	14922	15700	15079
$\bar{I}_{\text{body}}^{\text{yaw}}$ (period), kg m^2	1874	3155	1940	2321	3098	2478
ω_d , rad/s	5.01	4.81	4.99	4.94	4.83	4.92
ω_n , rad/s	5.02	4.82	5.01	4.95	4.84	4.93
ζ	0.063	0.069	0.077	0.055	0.051	0.063

pitch and roll tests had been conducted at relatively low displacements (maximum 0.02m), higher displacements occurred in the yaw case (maximum 0.1m) and the spring coefficient was considerably lower. Accurate characterising of springs is thus necessary and the effect of non-linearity should be taken into account in calculations of the period-related moment-of-inertia calculations.

The value of the yaw moment of inertia was also extremely sensitive to the measurement of the centre of gravity of the vehicle body (see Table 7). Due to the large contribution of the yaw moment of inertia about the rotational axis, I_o , to the body moment of inertia, $\bar{I}_{\text{body}}^{\text{yaw}}$, (equation 17 and Table 7) any effect that causes a small variation in the calculation of I_o (such as the measurement of the period or spring coefficient) causes a severe error in the calculation of $\bar{I}_{\text{body}}^{\text{yaw}}$. Also, for the experimental configuration used, the product of the vehicle body mass and the square of



Fig. 15 *Stabilising the vehicle against roll was necessary for determining yaw moment of inertia.*

the distance of the body centre of gravity to the pivoting point constitutes two-thirds of the value of I_o . Better results could thus be anticipated if the pivoting point had been at least at the height of the body centre of gravity, which would also prevent a rolling tendency.

General discussion of results

The discrepancy between the moments of inertia about the pivoting point obtained by means of the gradient of the torque–angular acceleration curve and that obtained

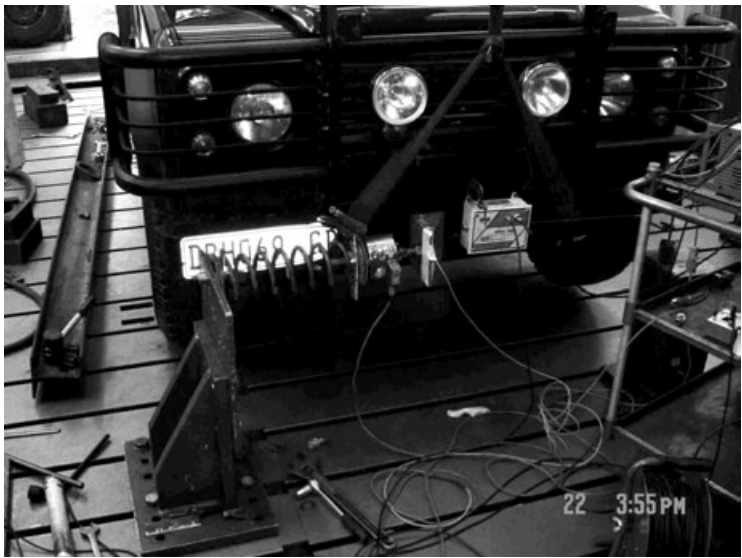


Fig. 16 *Positioning of the spring, load cell and displacement sensor in determining yaw moment of inertia.*

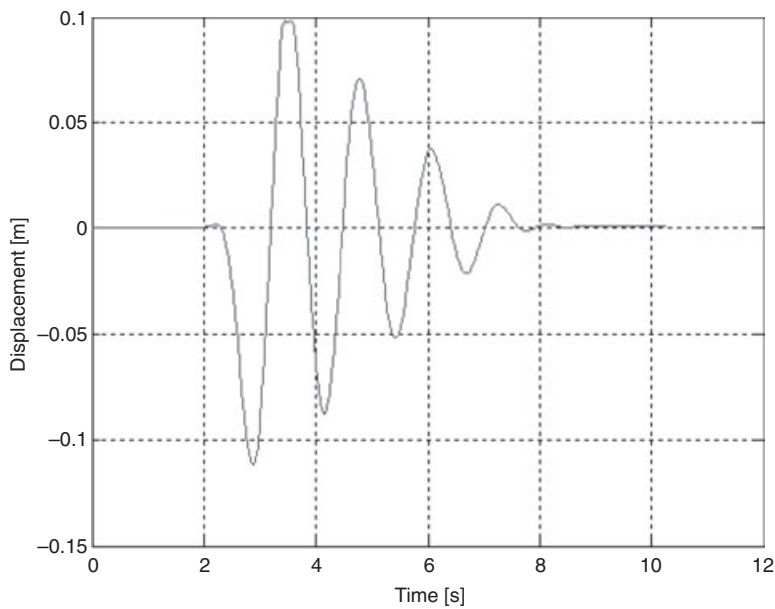


Fig. 17 *In determining yaw moment of inertia considerably more damping was present.*

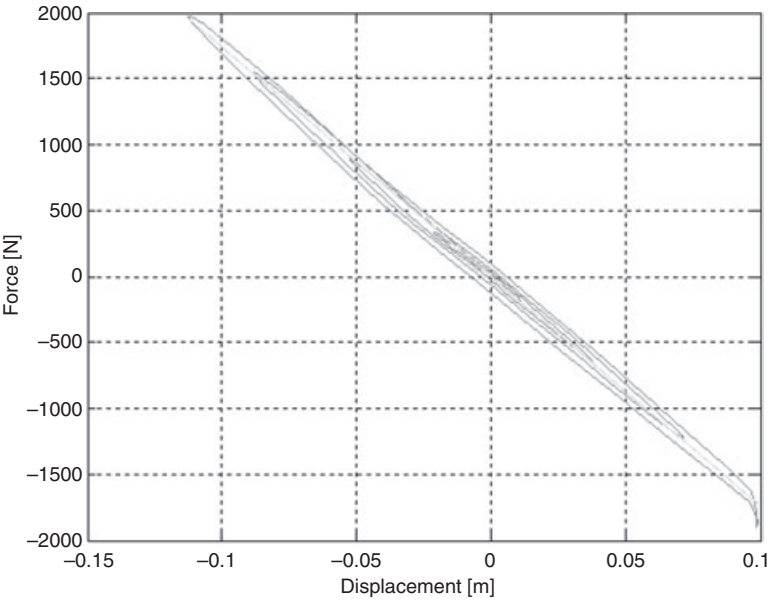


Fig. 18 Spring characteristics derived from displacement transducer and load cell.

TABLE 7 Sensitivity of yaw moment-of-inertia calculations to parameter variation

Parameter varied	Baseline value	10% deviation in I_o (acc)	10% deviation in $L_{\text{rotax_cog_body}}$	10% deviation in k	10% deviation in L_{force}	10% deviation in ω_d
I_o (accelerometer)	14029	10	0	0	0	0
$\tilde{I}_{\text{body}}^{\text{yaw}}$ (accelerometer)	1428	98	−147	0	0	0
I_o period spring	14476	0	0	10	21	−17
$\tilde{I}_{\text{body}}^{\text{yaw}}$ period spring	1874	0	−112	77	162	−134
ω_d	5.0127	0	0	0	0	10
ω_h	5.0226	0	0	0	0	10
$L_{\text{rotax_cog_body}}$	2.5235	0	10	0	0	0
L_{force}	4.6	0	0	0	10	0
k	17258	0	0	10	0	0

by means of the oscillation period has been observed to range from 2.6% to 11%. The discrepancy is ascribed to the effect of friction not being taken into account when the torque–angular acceleration curve is used. Use of the period method is recommended. Factors that have been observed to impact considerably on the accuracy of the calculations are measurements of distances and accurate determination of the position of the centre of gravity. In view of the effort and costs involved, the experiment has been successful in determining the values of the moments of inertia.

Implementation of these values on the simulation model has indeed led to an improvement between simulated and measured values.

Conclusions

Two methods to determine the moments of inertia of a two-ton vehicle in a standard university mechanical engineering laboratory have been investigated. In view of the effect of the friction moment, measuring the period of pitch, yaw or roll oscillation about a pivoting point is believed to be a more reliable approach than obtaining the moment of inertia from the gradient of the torque–angular acceleration curve. A difference of around 3% for determining moments of inertia about the pivoting point was obtained in the case of yaw and roll, and 11% in the case of pitch. The equipment necessary when using the oscillation period includes a load cell, a displacement transducer, a suitably characterised spring and data-processing equipment. An overhead crane can facilitate the various mounting requirements and determination of the centre of gravity. If practical considerations require that the pivoting point be distant from the centre of gravity, special heed must be taken in the measurement of distances. Since moments of inertia are calculated in terms of distances squared, small errors quickly escalate. This is further amplified by the fact that the squared distances are multiplied by large masses.

References

- [1] P. S. Els, 'The applicability of ride comfort standards to off-road vehicles', *Journal of Terramechanics*, **42** (2005), 47–64.
- [2] A. J. Scarlett, J. S. Price and R. M. Stayner, 'Whole body vibration: evaluation of emission and exposure levels arising from agricultural tractors', in *Proc. 9th European ISTVS Conference*, 8–11 September 2003 (Harper-Adams, UK, 2003), pp. 450–459.
- [3] P. L. Ringeoni, M. D. Actis and A. J. Patanella, 'An experimental technique for determining mass inertial properties of irregular shape bodies and mechanical assemblies', *Measurement*, **29** (2001), 63–75.
- [4] C. Shedlinski and M. Link, 'A survey of current inertia parameter identification methods', *Mechanical Systems and Processing*, **15**(1) (2001), 189–211.
- [5] H. A. Soulé and M. P. Miller, 'The experimental determination of the moments of inertia of air-planes', at <http://larc.nasa.gov/reports/1934/naca-report-467>, accessed February 2004.
- [6] A. Matsuo, H. Ozawa, K. Goda and T. Fukunaga, 'Moment of inertia of whole body using oscillating table in adolescent boys', *J. Biomechanics*, **28**(2) (1995), 219–223.
- [7] J. Wu and M. Hsieh, 'An experimental method for determining the frequency-dependent added mass and mass moment of inertia for a floating body in heave and pitch motions', *Ocean Engineering*, **28** (2001), 417–438.
- [8] D. A. Andreatta, G. J. Heydinger, R. A. Bixel and D. A. Coover, 'Inertia measurements of large military vehicles', *Transactions of the SAE*, technical note 2001-01-079 (2001).
- [9] G. J. Heydinger, D. J. Durisek, D. A. Coover, D. A. Guenther and S. J. Novak, 'The design of a vehicle measurement facility', *Transactions of the SAE*, 950309 (1995).
- [10] R. A. Bixel, G. J. Heydinger, N. J. Durisek, D. A. Guenther and S. J. Novak, 'Developments in vehicle centre of gravity and inertial parameter estimation and measurement', *Transactions of the SAE*, 950356 (1995).
- [11] D. D. MacInnis, W. E. Cliff and K. W. Ising, 'Comparison of moment of inertia estimation techniques for vehicle dynamics simulation', *Transactions of the SAE*, 9709051 (1997).

- [12] C. Doniselli, M. Gobbi and G. Mastinu, 'Measuring the inertia tensor of vehicles', *Vehicle System Dynamics Supplement*, **37** (2002), 301–313.
- [13] R. S. Sharp, 'Measurment of mass and inertial properties of vehicles and components', *Autotech*, C524/145/97 (1997).